

# Wall Compensation for Ultra Wideband Applications

Ali H. MUQAIBEL, Nuruddeen M. IYA, Umar M. JOHAR

Dept. of Electrical Engineering, King Fahd Univ. of Petroleum & Minerals, P.O. Box 1734, Dhahran 31261, Saudi Arabia

muqaibel@kfupm.edu.sa, nuruddeeniya@yahoo.com, umjohar@kfupm.edu.sa

**Abstract.** *Due to their low frequency contents, ultra wideband (UWB) signals have the ability to penetrate walls and obstacles. As the signal propagates through these obstacles, it gets attenuated, slows down, and gets dispersed. This paper demonstrates wall compensation for through-wall imaging, localization and communication receiver design purposes by first characterizing wave propagation through various building materials in the UWB frequency range. Knowledge of the walls obtained from the wall characterization is used to estimate and correct the position accuracy of a target object located behind the walls using three proposed methods namely; constant amplitude and delay (CDL), frequency dependent data (FFD), and data fitting methods (FIT). The obtained results indicated relatively acceptable measure of wall compensation for the three methods. Results from such work provide insight on how to develop algorithms for effective target position estimation in imaging and localization applications. They are also useful for channel modeling and link budget analysis.*

## Keywords

Wall compensation; localization; UWB; through-wall imaging.

## 1. Introduction

Electromagnetic waves passing through a medium are subject to amplitude and phase distortions. These distortions are attributed to dispersive and attenuative properties of the medium of propagation. A propagation path obstruction is defined as a man-made or natural physical object that lies close enough to a radio wave path to cause a measurable effect on the path loss exclusive of reflection effects [1]. There is an increasing need to understand and model electromagnetic effects associated with wave propagation through obstacles. In addition to materials that make the wall, the shape of the wall, its composition, multiple reflections within the wall, angles of incidence on the wall, coupling effects, radiation pattern, and polarization of transmit and receive antennas are important factors that need to be taken into consideration.

Several studies have been conducted on the electromagnetic characterization of building materials both in the

narrowband [2]–[5], and wideband [6]–[7] ranges of frequencies. Electromagnetic parameters including insertion loss, dielectric constant, loss tangent, reflection and transmission coefficients were used to present wall characteristics. Research has been done to propose methods to mitigate the effect of walls on signal propagation and target detection. Chandra et al. [8] applied a singular value decomposition algorithm to minimize clutter and detect a metallic target behind plywood and brick wall in the UWB frequency range. In [9], Guolong et al. illustrated the impact of delay in position accuracy and used a through-the-wall compensation algorithm to correct the position of the located human to within 24 cm. Ahmad et al. [10] demonstrated the imaging problem with practical assumptions of unknown wall parameters. They proposed an auto-focusing technique based on higher order statistics that provides high quality images with locations close to true target locations. Rovnakova et al. [11] proposed two methods to correctly trace moving targets behind walls and compensate for the ‘wall effect’.

Imaging accuracy, however, is not only dependent on signal processing but also on the availability of detailed information about buildings, which includes material constants (permittivity and conductivity), thicknesses of walls, as well as the structures of the buildings themselves [12]. In this paper, we investigate the obstruction effect and propose methods to compensate for the effect. This is achieved by first performing a wideband electromagnetic characterization of typical building wall materials and assessing their impacts on localization. Measurements are carried out on samples of wood, glass and gypsum walls to characterize them over a frequency range of 1–18 GHz using a vector network analyzer. The characterization method is based on measuring the *insertion transfer function*, defined as the ratio of two signals measured in the presence and in the absence of the wall. The dielectric constant of the wall material is related to the measured insertion transfer function through a complex transcendental equation that can be solved using an approximate one-dimensional root search [13]. Transmission and reflection measurements were carried out in frequency domain using free space radiated measurement to extract the insertion loss and dielectric constant for each wall material. Free space radiated measurements are contactless and non-destructive. They also match the configuration of the final application for which the measurements are carried out, which is radar and communication.

While penetrating through a material, an electromagnetic wave for through wall imaging and detection may change its speed significantly. This is closely related to the wall thickness and composition, its dielectric constant, and the angle of incidence of the wave. In addition to slowing down, the signal gets attenuated and undergoes refraction as it passes through the wall. It defocuses target image and displaces the target from its true position. False targets can also be present in the radar images. These effects are more pronounced for walls with higher dielectric constants or in presence of multiple walls between target and radar [10]. Wall compensation therefore, is when effort is being made to correct the adverse effect of the wall on the outcome of the detection process so that the true target position can be obtained. This work attempts wall compensation by using wall information obtained from the wall characterization to correct the position estimation of the target object. This is achieved through conducting target experiments.

When compensating for the wall effect, we either use full frequency dependent data or approximate fits. Three possibilities are proposed and compared. The first method employs constant amplitude loss and delay suffered by the signal as obtained from previous wall characterization measurements to compensate for the wall effect in the target measurements. The second method uses previously known frequency dependent wall information represented by magnitude and phase data, while the third method which is a trade-off between the first two uses linear and quadratic fits to magnitude of the insertion loss and dielectric constants of the wall respectively.

This paper is organized as follows. Section 2 summarizes the wall characterization process and results. Section 3 describes the experimental setup and procedure for the target measurements. In section 4, the proposed wall compensation methods are explained and the results from each method are illustrated. Finally, concluding remarks about the work are given in section 5.

## 2. Wall Characterization

Both magnitude and phase information are needed for accurate characterization of walls. Using the frequency domain technique, complex data points representing magnitude and phase information are obtained. These data are obtained using vector network analyzer.

The insertion transfer function is obtained as the ratio of two transmit signals given as [5]

$$H(j\omega) = \frac{X_t(j\omega)}{X_t^{fs}(j\omega)} \tag{1}$$

where  $X_t^{fs}(j\omega)$  and  $X_t(j\omega)$  are ‘free-space’ reference and ‘through-wall’ frequency domain signals obtained in the absence and presence of the wall respectively. The ‘free-space’ measurement is used as reference to take care of the effects of components other than the wall. Extra

caution should be taken to make sure that exact setup is used to perform both experiments in order to avoid measurement inconsistencies.

Assuming a fictitious layer of free-space of the same thickness as the wall, then the propagation delay through this layer is  $\tau_0 = d/c$  where  $d$  is the layer thickness and  $c$  is the speed of light in free space. The scattering parameter related to the insertion transfer function in this case is given as

$$S_{21}(j\omega) = H(j\omega)e^{-j\omega\tau_0} \tag{2}$$

The un-gated insertion transfer function is obtained by dividing the through wall  $S_{21}$  data by that of free space. A finite impulse response filter is then used to remove the noise at the low frequencies and those beyond the antenna bandwidth. The frequency domain signals are then converted to time domain using inverse fast Fourier transform to get the impulse responses. Zeros are padded for higher time domain resolution. The impulse responses obtained from frequency-domain measurements are correlated using a sliding correlator to obtain the first guess on the delay and effective dielectric constant. An estimate of the average dielectric constant could also be obtained through peak-to-peak impulse time delay,  $\Delta\tau$ . This average dielectric constant, which does not reflect the frequency dependence, is given by

$$\epsilon_r' \cong \left[ 1 + \frac{\Delta\tau}{d/c} \right]^2 \tag{3}$$

As a function of the unwrapped phase,  $\Phi_{sp}(f)$ , the dielectric constant is also given by

$$\epsilon_r'(f) \cong \left[ 1 + \frac{\Delta\tau(f)}{\tau_0} \right]^2 = \left[ 1 - \frac{\Phi_{sp}(f)}{2\pi\tau_0 f} \right]^2 \tag{4}$$

	Coefficients of linear or quadratic fits to extracted parameters – $af + b$ or $af^2 + bf + c$ , $f$ (GHz)								
	Wood			Glass			Gypsum		
	<i>a</i>	<i>b</i>	<i>c</i>	<i>a</i>	<i>b</i>	<i>c</i>	<i>a</i>	<i>b</i>	<i>c</i>
Insertion transfer function	-0.245	-0.785	--	-0.0424	-1.687	--	-0.0175	-0.462	--
Dielectric constant	0.0016	-0.056	3.157	-0.910	8.0396	--	0.0008	-0.0257	2.83

Tab. 1. Coefficients for extracted parameters.

In the absence of an anechoic chamber, multipath components, multiple reflections in the wall, and reflections from the floor, ceiling and other structures become a threat to the measurement accuracy. In order to reduce this effect of multipath, time gating is used to selectively

remove or include the undesired responses in time. The remaining time domain responses can then be transformed back to the frequency domain with the effect of the ‘gated-out’ responses being removed. The delayed signals can be filtered out by imposing a window function over the dominating signal that is identified to be the desired one. The gated insertion transfer function is then obtained from which the dielectric constant is calculated using the multiple pass technique from [13]. Fig. 1 shows the results for the insertion transfer function and dielectric constants respectively for wood, glass and gypsum walls. The coefficients for these results are shown in Tab. 1.

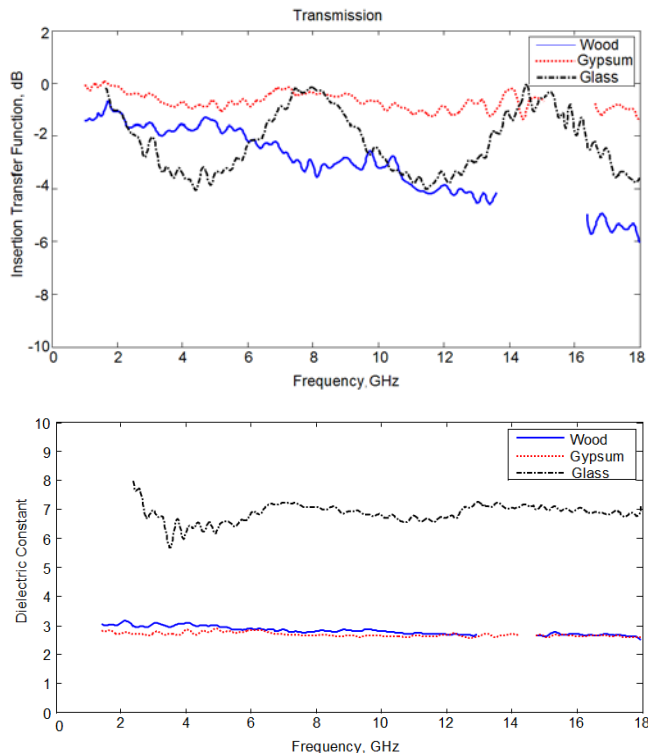


Fig. 1. Magnitude of insertion transfer function (upper). Dielectric constant (lower).

### 3. Measurement Setup and Procedure

An HP8510C vector network analyzer with two-port  $S$ -parameter test set was used to perform target measurements within the band of interest. The output of the network analyzer port 1 is fed through a 1.5 m cable to a wideband power amplifier; another 1.5 m cable connects the amplifier output to a wideband horn antenna mounted on a tripod. An identical antenna mounted on a similar tripod stand is used as a receiving antenna. The receive antenna output is fed to the network analyzer port 2. An aluminum sheet is used as the target object because it approximately reflects all the energy impinging on its surface.

The procedure is as follows. The aluminum sheet (target) is put in front of both antennas at a given distance.

A transmitted signal from the transmitter is reflected by the aluminum and received by the receiving antenna. This is the reference measurement or ‘Target Only’. A wall is then inserted between the antennas and the target with some distance on both sides as shown in Fig. 2 and another measurement is carried out. The steps above were repeated for wood, glass, gypsum, and some multiple wall combinations. In each case, frequency domain responses are acquired.



Fig. 2. Through target measurements setup.

Fig. 3 shows the processed bandlimited time-domain impulse response from the target both with and without a wood wall. There are two main reflections in the case of the target behind the wall. The first (early) response (solid line) indicates a reflection from the wall surface. We can clearly see a delayed and attenuated response from the target when it is behind the wall represented by the second reflection. This delay translated into distance, corresponds to shift in the actual position of the target behind the wall. The dotted line represents the ‘Target Only’ measurement.

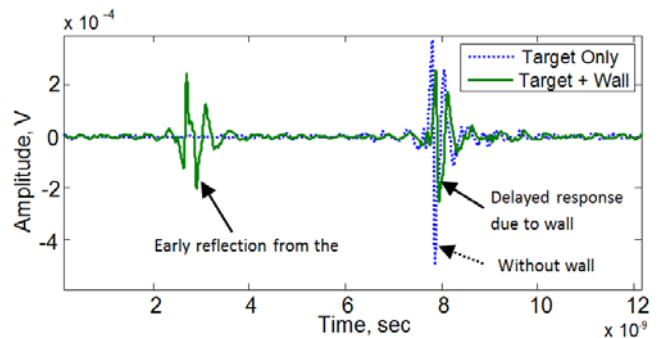


Fig. 3. Reflections from target object with and without obstruction.

### 4. Wall Compensation Methods

The objective is to compensate for the target displacement by removing the effect of the wall on the response obtained from the target. This is achieved in three different methods: (1) Using constant amplitude and delay (CDL), (2) Using full frequency dependent raw data (FFD), and (3) Using fitted dielectric constant and fits to the magnitude of frequency dependent data (FIT).

### 4.1 Constant Amplitude and Delay Compensation

In the constant amplitude and delay compensation, it is assumed that there is constant amplitude attenuation due to the wall. It is also assumed that the delay is constant and thus, there is no frequency dependence. For each wall, we use the amplitude attenuation it incurred during wall characterization as ‘constant amplitude’ to compensate for the amplitude loss the same wall suffered in the target measurements. A similar approach is performed on the delay, and the time is corrected by a value equal to the delay the wall offered during the wall characterization measurements. Tab. 2 shows the constant values used for amplitude and delay compensation. Fig. 4 shows the compensated signal using this approach compared with the response obtained without a wall for the case of wood, glass, and gypsum. The constant amplitude used information from transmission measurements, while the constant delay used is twice the value of the delay from transmission measurements. This is because the reflection measurement requires the signal to propagate twice through the wall.

Wall	Constant amplitude	Constant delay (ns)
Wood	1.44	0.08513
Glass	1.24	0.0864
Gypsum	1.104	0.0690

Tab. 2. Constant amplitude and constant delay values used.

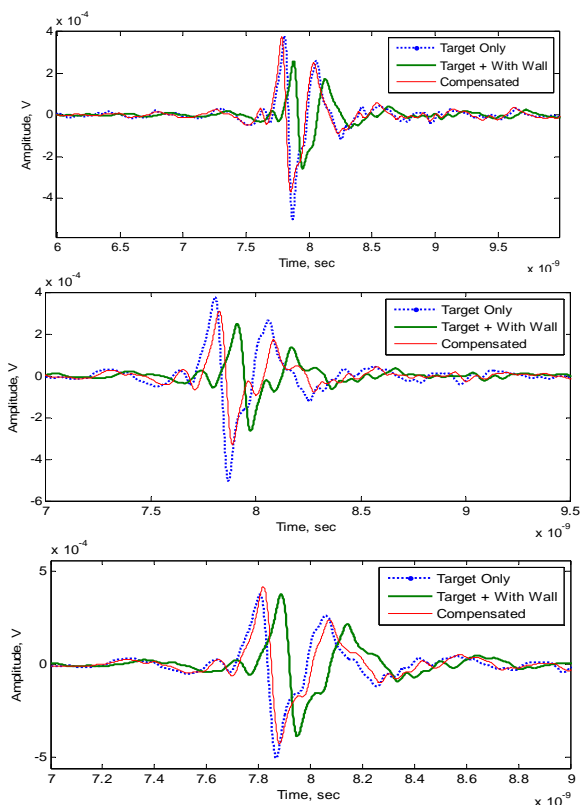


Fig. 4. Illustrating compensation using constant amplitude and constant delay, wood (upper), glass (middle), gypsum (lower).

### 4.2 Frequency Dependent Data Method

For more accurate determination of the target’s position, the frequency dependent effect of the wall has to be removed. This is achieved by dividing total transfer function by that of the wall. This is achieved using our previous knowledge of the wall obtained from wall characterization. Fig. 5 shows the result for wood both in frequency and time domain. Similar results were obtained for other walls but are not presented here due to the limited space.

It should be noted that because of the raw frequency domain data directly obtained from measurements, the presence of noise is a major concern. Noise clearly manifests in the time domain. Therefore, noise reduction is performed by filtering the noisy regions around 1 GHz and 15.5 GHz as in Fig. 5.

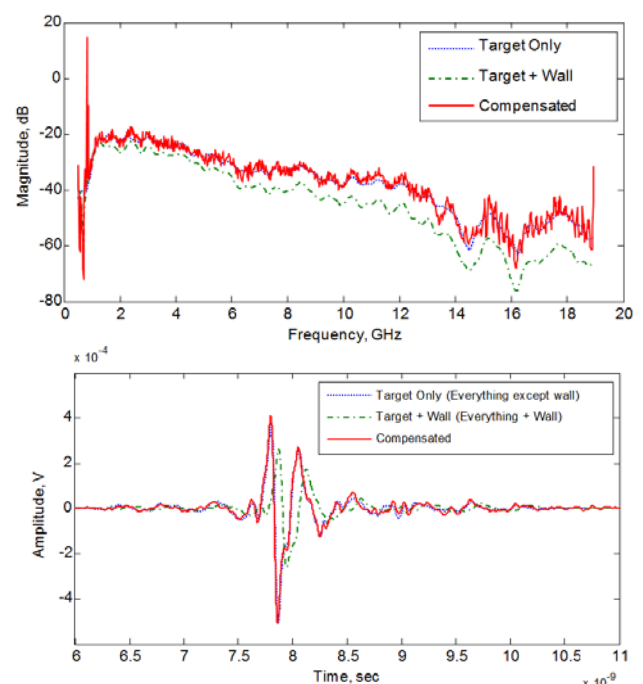


Fig. 5. Wall compensation using raw data for wood sample in frequency domain (upper), and time domain (lower).

There is a close agreement between the compensated responses and the responses obtained from measurements performed without the wall. The advantage of this method over compensating with a constant delay and amplitude is that the pulse shape is corrected. In application like matched filter or correlation receivers, pulse shape correction is very important. The cost will be to provide a full data about the insertion transfer function of the wall.

### 4.3 Data Fitting Method

As a trade-off between the above two methods, one can provide the parameters that model the magnitude of the insertion loss of the wall using a linear equation to reflect the frequency dependence of the magnitude of the transfer function. Higher order fits are also possible but not needed especially if the walls used are having some variability.

In this method, the result of the dielectric constant given in Tab. 1 is used to obtain an un-wrapped phase  $\Phi_w$  from (4). The delay  $\tau_o$  is still modeled with a constant value as in the case with constant amplitude and delay method. The phase obtained is then used together with the results of the magnitude of insertion transfer function (having coefficients in Tab. 1, to calculate a complex insertion transfer function  $H_w(f) = |H_w(f)| \exp[j\Phi_w(f)]$  representing the wall. The result for compensation using this method for wood and glass is shown in Fig. 6. Wood shows good wall compensation as indicated by the similarity between the ‘Target Only’ and ‘Compensated’ responses. The compensation for glass did not show good results.

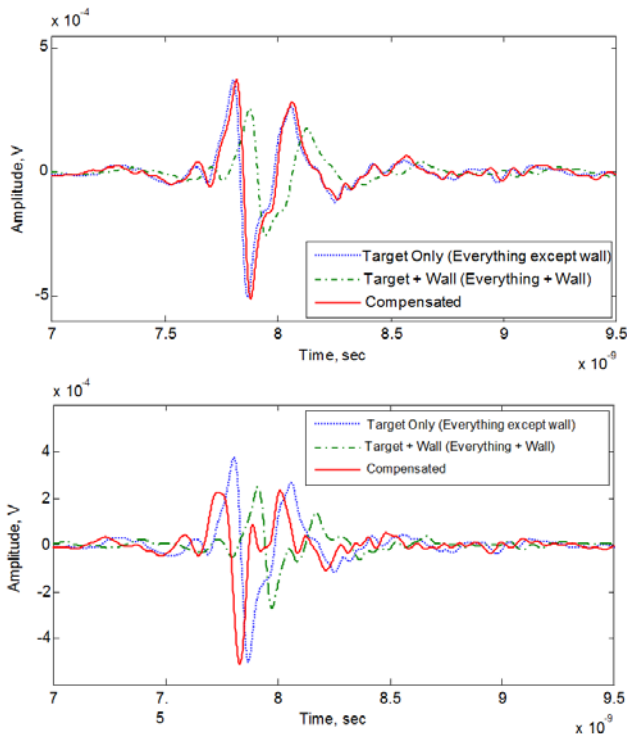


Fig. 6. Wall compensation using fit to data for wood (upper), and glass (lower)

#### 4.4 Performance Evaluation for the Suggested Wall Compensation Methods

In order to assess the accuracy of the methods mentioned above in achieving wall compensation, we will make comparison between results for ‘No Wall’ and that of ‘Compensated’ (estimate). We also compare these results with the case where there is no compensation. The comparison will be in terms of the delay (peak-to-peak) and energy capture.

The peak-to-peak delay is useful in positioning applications and can be used to give approximate errors in the true position of detected objects. Since time and distance are related by the expression

$$s = v \Delta \tau \quad (5)$$

where  $v = c/\sqrt{\epsilon_r'}$  is the velocity of the wave through the

wall of dielectric constant  $\epsilon_r'$ , the speed of light,  $c = 3.0 \cdot 10^8$  and  $\Delta \tau$  is the peak-to-peak time delay incurred by the signal passing through the wall. The dielectric constant  $\epsilon_r'$  can be a value chosen at the mid-frequency range for the wall material under consideration.

Tab. 3 provides errors in delay corresponding to approximate errors in the position of the target due to the three different walls. It also shows approximate errors after compensation has been done for the three methods.

For the purpose of Tab. 3, we refer to the three methods with the following abbreviations in parenthesis: Constant Amplitude and Delay (CDL), Frequency Dependent Data (FFD), Fitted Dielectric constants and Fits to Magnitude of Frequency Dependent Data (FIT), and ‘No Compensation’ as (NC).

Wall	Thickness (cm)	$\epsilon_r'$	Peak-to-peak error (ns)			
			Due to wall	After compensation		
				NC	CDL	FFD
Wood	1.8	3.0	0.07094	-0.01489	-0.00645	0.01161
Glass	0.8	6.5	0.10577	0.01936	0.02193	-0.0606
Gypsum	1.2	2.4	0.08126	0.01225	0.03224	-0.0116

Tab. 3. Constant amplitude and constant delay values used.

Since time domain responses are used to demonstrate wall compensation, the peak-to-peak delay was used to find the error due to the wall by comparing the ‘Target Only’ and ‘Target +Wall’ responses. Similarly, the peak-to-peak delay for the ‘Target Only’ and ‘Compensated’ responses are used to get the error after compensating for the wall. An equivalent error in displacement is also obtained. The negative sign in the errors indicate instances where we have ‘over-compensation’; therefore, the peak-to-peak difference will be negative. Note that these figures depend on the dielectric constant and thickness of the walls.

Studying Tab. 3 closely, we can see that relative to no compensation at all (NC), wood perform better after FFD compensation as indicated by 0.0064 ns error in delay compared to 0.0148 ns and 0.0116 ns for CDL and FIT respectively. CDL gives 0.0193 ns error after compensation for glass which is less compared to that of FFD and FIT. Because peak-to-peak delay is used, changes in pulse shapes of the compensated responses for FFD and FIT will affect the amount of error both in time and space. We also attribute this to the high dielectric constant of glass, even though the thickness of our glass wall is 0.8 cm.

Recall that walls with higher dielectric constant tend to defocus target images introducing errors in target positions [9]. This will yield up to 0.71 cm error FIT compensation. For gypsum, FFD has the highest amount of error after compensation with 0.03224 ns relative to NC, followed by CDL with 0.01225 ns. FIT gives the least. Over-

all, CDL compensation seems to give less error for the three walls and wood gives a better error performance for all three methods.

Energy capture is useful when analyzing signal waveforms. For our purpose, we employ the energy capture equation described in [13] to be

$$EC = \left\{ 1 - \frac{\|r(t) - r_c(t)\|^2}{\|r(t)\|^2} \right\} \times 100\% \tag{6}$$

where  $r(t)$  is the ‘Target Only’ signal called the ‘true signal’, and  $r_c(t)$  is the ‘Compensated’ signal and it is called the ‘estimate of the true signal’. A window size of 1 ns around the main pulses is assumed. To achieve full comparison between the shapes of the waveforms, they are first synchronized, and then the estimate is subtracted from the true signal to get the difference. If the difference is greater than the true signal  $r(t)$ , the percentage energy capture will be negative.

Tab. 4 shows how similar, in percentage, the wall compensation results are to the results obtained from measurements without the wall for wood, glass and gypsum, using Constant Amplitude and Delay Method, Frequency Dependent Data Method, and Data Fitting Method. We have added a column representing when there is no compensation (between ‘Target Only’ and ‘Target + Wall’). It should be noted that the accuracy of these figures depends on the size of the window around the main pulse over which the comparison is made. Wood and gypsum showed good compensation particularly in the data fitting method. This is indicated by the 99.32% similarity to the ‘No Wall’ case for wood and 98.70% for gypsum. For glass, we have up to 16% improvement in the results from the frequency dependent data method (96.45%) over constant amplitude and delay’s 80.68%. However, in the data fitting method, compensated waveform for glass suffered considerable distortion. Overall, the results for energy capture in frequency dependent data method show relatively better similarity between ‘Target Only’ and ‘Compensated’ responses.

Wall	Method			
	No Compensation	Constant Amplitude and Delay	Frequency Dependent Data	Data Fitting
Wood	83.94 %	93.52 %	95.61 %	99.32 %
Glass	71.52 %	80.68 %	96.45 %	76.82 %
Gypsum	94.85 %	96.27 %	98.98 %	98.70 %

Tab. 4. Percentage similarity of wall compensation results to ‘No Wall’ results.

Generally, the basis of comparison depends on how the receiver is interested in the signal (time, energy, etc). Fig. 7 shows the three different methods compared for our wood wall. As with the matched filter system, the use of pulse peak-to-peak delay to measure the correlation between the two results might be an easier approach to take however; in this case, the shape of the waveform is affected during the compensation process. Therefore, finding the correct peak of the signal will not be easy and the peak-to-peak delay will yield an unreliable outcome which cannot represent correlation or similarity. Consequently, wall compensation for double and triple walls suffered severe change in waveform, thus, no reliable results were obtained for them. Fig. 8 shows an example for the case of double wall: wood-gypsum.

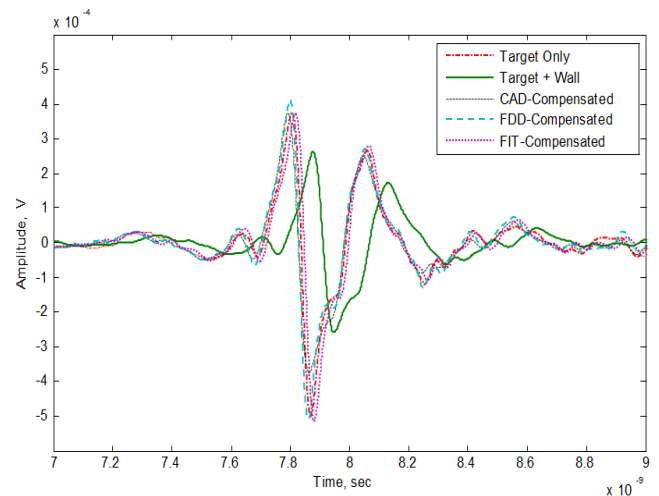


Fig. 7. Compensation using the three methods for wood wall.

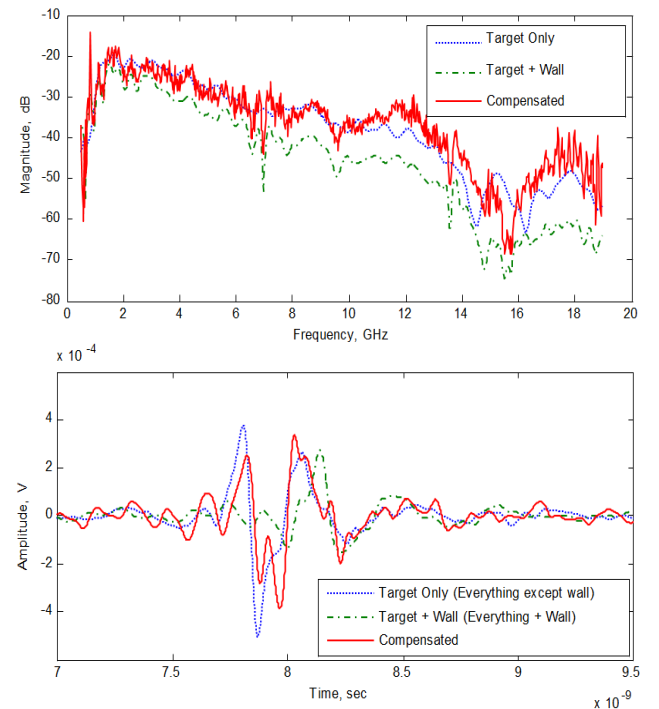


Fig. 8. Wall compensation for double wall (wood-gypsum). Frequency domain (upper), time domain (lower).

## 5. Conclusion

This paper proposes a way of compensating for the effect the obstruction has on the true position of a target in through wall detection applications. Three methods for wall compensation were discussed.

The first one used estimated constant amplitude loss and delay values suffered by the walls in the previous wall characterization experiments to perform compensation, while the second uses full frequency dependent data from previous knowledge of the wall. The third uses a quadratic and linear fit to previously obtained dielectric constant and magnitude of insertion loss respectively, while assuming a constant delay. Results obtained show a good level of wall compensation for the different walls used. Based on energy capture, results obtained show a good level of wall compensation for the different walls used. With the first method, up to 93.52% similarity was recorded between compensated and no wall responses for wood. Similarly, 98.70% similarity was obtained with the third method for gypsum wall.

## Acknowledgment

The authors would like to acknowledge the support provided by the Deanship of Scientific Research at King Fahd University of Petroleum & Minerals (KFUPM) and the King Abdul-Aziz City of Science and Technology (KACST) under Research Grant # NSTP: 08-ELE44-4-1. The authors would like also to thank Dr. Mohamed Adnan Landolsi, and Dr. Abdullah Al-Ahmari for their valuable input.

## References

- [1] TESSERAULT, G., MALHOUREUX, N., PAJUSCO, P. Determination of material characteristics for optimizing WLAN radio. In *Proceedings of the 10th European Conference on Wireless Technology*. Munich (Germany), 2007, p. 225 – 228.
- [2] OUSLIMANI, H. H., ABDEDDAIM, R., PRIOU, A. Free-space electromagnetic characterization of materials for microwave and radar applications. *Progress in Electromagnetics Research Symposium*. Hangzhou (China), 2005, p. 128 – 132.
- [3] AKUTHOTA, B., ZOUGHI, R., KURTIS, K. E. Determination of dielectric property profile in cement-based materials using microwave reflection and transmission properties. In *Instrumentation and Measurement Technology Conference*. Como (Italy), 2004, p. 327 – 332.
- [4] CUINAS, I., SANCHEZ, M. Measuring, modelling, and characterizing of indoor radio channel at 5.8 GHz. *IEEE Transactions on Vehicular Technology*, 2011, vol. 50, no. 2, p. 526 – 535.
- [5] MUQAIBEL, A., SAFAAI-JAZI, A., BAYRAM, A., ATTIYA, A., RIAD, S. Ultrawideband through-the-wall propagation. *IEE Proceedings on Microwave Antennas Propagation*, 2005, vol. 152, no. 6, p. 581 – 588.
- [6] LIU, C., HUANG, C., CHIU, C. Channel capacity for various materials of partitions in indoor ultra wideband communication system with multiple input multiple output. In *3rd IEEE UZ Regional Chapter International Conference in Central Asia on Internet*, Taskent (Uzbekistan), 2007, p. 1 – 5.
- [7] CHANDRA, R., GAIKWAD, A., SINGH, D., NIGAM, M. An approach to remove the clutter and detect the target for ultra-wideband through-wall imaging. *Journal of Geophysics and Engineering*, 2008, vol. 5, p. 412 - 419.
- [8] CUI, G., KONG, L., YANG, J., WANG, X. A new wall compensation algorithm for through-the-wall radar imaging. In *1st Asian and Pacific Conf. on Synthetic Aperture Radar*, 2007, p. 393–396.
- [9] AHMAD, F., AMIN, M. G., MANDAPATI, G. Autofocusing of through-the-wall radar imagery under unknown wall characteristics. *IEEE Transactions on Image Processing*, 2007, vol. 16, p. 1785 - 1795.
- [10] ROVNAKOVA, J., KOCUR, D. Compensation of wall effect for through-wall tracking of moving targets. *Radioengineering*, 2009, vol. 18, no. 2, p. 189 – 195.
- [11] YI, H., PARSONS, D. A time domain approach for measuring the dielectric properties and thickness of walls of a building. In *IEE Colloquium on Propagation aspects of Future Mobile Systems*. 1996, p. 7/1 – 7/7.
- [12] MUQAIBEL, A., SAFAAI-JAZI, A. A new formulation for characterization of materials based on measure insertion transfer function. *IEEE Transactions on Microwave Theory and Techniques*, 2003, vol. 51, no. 8, p. 1946 – 1951.
- [13] WIN, M., SCHOLTZ, R. Energy capture vs correlator resources in ultra-wide bandwidth indoor wireless communications channels. In *MILCOM '97 Proceedings*. 1997, vol. 3, p. 1277 – 1281.

## About Authors ...

**Ali MUQAIBEL** was born in Dammam, Saudi Arabia in 1974. He received his B.Sc. and M.Sc. from King Fahd University of Petroleum & Minerals (KFUPM) in 1996 and 1999, respectively. He obtained his Ph.D. from Virginia Polytechnic Institute and State University (Virginia Tech) in 2003. He is currently an Associate Professor at the Electrical Engineering Department at KFUPM. His research interests include Ultra Wideband (UWB) communications, channel modeling, positioning, and compressive sensing techniques. He is the author or co-author of about 40 papers published in scientific journals or conference proceedings.

**Nuruddeen IYA** was born in Yola, Nigeria. He obtained his M.Sc. from King Fahd University of Petroleum & Minerals (KFUPM) in 1996. His research interests include ultra wideband (UWB), and through wall propagation.

**Umar JOHAR** was born in February 1967. He received his B.Sc. and M.Sc. degrees from the King Fahd University of Petroleum & Minerals (KFUPM), Saudi Arabia in 1990 and 1993 respectively. He worked as a Research Assistant in the Electrical Engineering Department at KFUPM from November 1990 to January 1993. In February 1993, he joined the same department to work as a Lecturer where he is still employed. His research interest includes electromagnetics, fiber optics, microwave engineering, wireless communications and UWB.